THE UNIVERSITY OF
WARWICK

Original citation:
Rahmanpour, Rahman , Rea, Dean, Jamshidi, Shirin, Fulop, Vilmos and Bugg, Timothy D. H.. (2016) Structure of Thermobifida fusca DyP-type peroxidase and activity towards kraft lignin and lignin model compounds. Archives of Biochemistry and Biophysics, 594 . pp. 54-60.

Permanent WRAP url:
http://wrap.warwick.ac.uk/77595

warwick**publications**wrap

highlight your research

http://wrap.warwick.ac.uk/

Structure of *Thermobifida fusca* DyP-type Peroxidase and Activity towards Kraft Lignin and Lignin Model Compounds

Rahman Rahmanpour[a], Dean Rea[b], Shirin Jamshidi[a], Vilmos Fülöp[b], and Timothy D. H. Bugg[a]*

Department of Chemistry[a] and School of Life Sciences[b], University of Warwick,

Gibbet Hill Road, Coventry CV4 7AL, UK

*Author for correspondence. Address: Department of Chemistry, University of Warwick, Coventry

CV4 7AL. Email T.D.Bugg@warwick.ac.uk, Tel 44-2476-573018

Abstract: A Dyp-type peroxidase enzyme from thermophilic cellulose degrader *Thermobifida fusca* (TfuDyP) was investigated for catalytic ability towards lignin oxidation. TfuDyP was characterised kinetically against a range of phenolic substrates, and a compound I reaction intermediate was observed via pre-steady state kinetic analysis at λ_{max} 404 nm. TfuDyP showed reactivity towards Kraft lignin, and was found to oxidise a β-aryl ether lignin model compound, forming an oxidised dimer. A crystal structure of TfuDyP was determined, to 1.8Å resolution, which was found to contain a diatomic oxygen ligand bound to the heme centre, positioned close to active site residues Asp-203 and Arg-315. The structure contains two channels providing access to the heme cofactor for organic substrates and hydrogen peroxide. Site-directed mutant D203A showed no activity towards phenolic substrates, but reduced activity towards ABTS, while mutant R315Q showed no activity towards phenolic substrates, nor ABTS.

Keywords: dye decolorizing peroxidase; Dyp; lignin oxidation; protein crystallography

Introduction

The dye-decolorizing peroxidases (DyPs) are a class of heme peroxidase enzyme found in bacteria and fungi, that have a different structural fold to other classes of heme peroxidase, and which show particular reactivity for oxidation of polycyclic dyes, as well as phenolic compounds [1,2]. They contain an active site aspartic acid residue that is believed to function as a proton donor, for generation of the compound I intermediate for substrate oxidation [3]. Although first discovered in fungi [4], they are found in a range of bacteria, and have been classified on the basis of phylogenetic analysis into four sub-classes DyPA-D [5]. A-type DyPs from *Bacillus subtilis* [6] and *Rhodococcus jostii* [7] show peroxidase activity towards anthraquinone dye and phenolic substrates, but *E. coli* enzymes YfeX and EfeB in the DyPA sub-family have also been shown to catalyse heme deferrochelation activity [8]. B-type DyPs also show activity towards anthraquinone dyes and phenolic substrates, but *Rhodococcus jostii* DypB has been shown to oxidise a lignin β-aryl ether model compound and Mn^{2+}, and in the presence of Mn^{2+} shows oxidation activity towards polymeric lignin [9]. C-type DyPs such as DyP2 from *Amycolatopsis* sp. 75iv2 show much higher oxidation activity towards Mn^{2+}, comparable to fungal Mn peroxidase enzymes, and can decolorize Reactive Black 5, a dye substrate with a high redox potential [10]. D-type DyPs, found in fungi such as *Bjerkandera adusta* [11] and *Auricularia auricular-judae* [12], show high activity towards phenolic substrates and ABTS, and also show activity towards high-redox potential dyes.

The identification of bacterial enzymes such as *R. jostii* DyPB for lignin oxidation [9] offers the potential to use bacteria to valorise lignin, a recalcitrant aromatic polymer found in plant lignocellulose, and produced by pulp/paper manufacture and cellulosic bioethanol production [13]. We have shown that a vanillin dehydrogenase gene deletion mutant of *R. jostii* RHA1 is able to accumulate vanillin, a high value aromatic product, when grown in minimal media containing wheat straw lignocellulose as carbon source [14]. We have also identified a B-type DyP in *Pseudomonas fluorescens* with activity for oxidation of lignocellulose in the presence of Mn^{2+}, thereby generating a lignin dimer product [15]. A DyP-type peroxidase has also been reported from

2

Thermobifida fusca, a thermophilic cellulose degrader, which was shown to have activity towards a range of phenolic and anthraquinone dye substrates, and to catalyse enantioselective sulfoxidation reactions [16]. Since *T. fusca* will encounter the lignin polymer during cellulose degradation, we wanted to examine whether the *T. fusca* DyP has peroxidase activity towards lignin. In this paper we report the kinetic characterisation of TfuDyP towards lignin substrates, the determination of its crystal structure, and an investigation of the function of active site residues.

Materials and Methods

Expression of recombinant TfuDyP

Genomic DNA was extracted from *Thermobifida fusca* yx using the Wizard genomic DNA purification kit (Promega), using the manufacturer's instructions. The *T. fusca* gene (accession number Q47KB1) was amplified from genomic DNA by polymerase chain reaction using the following oligonucleotide primers: forward 5'-ATGACCGAACCAGACACGG-3'; reverse 5'-TCATCCTTCGATCAGGTCCTG-3'. The amplified 1293 bp gene was cloned into expression vector pET151 using the Champion pET151 Directional TOPO Expression Kit (Invitrogen) using manufacturer's instructions, and transformed into *E. coli* TOP10 competent cells (Invitrogen). The sequence of the cloned gene was confirmed by DNA sequencing, and the recombinant plasmid was transformed into *E. coli* BL21 (Invitrogen) for protein expression. A TEV recognition site (Glu-Asn-Leu-Tyr-Phe-Gln-Gly) and its downstream sequence was encoded in the expression vector before the Met starting codon. After TEV protease cleavage, the scar peptide Ile-Asp-Pro-Phe-Thr remains connected to the N terminus of TfuDyP protein.

Purification & reconstitution of recombinant TfuDyP

A 2 litre culture of *E. coli* BL21/pET151(TfuDyP) was grown in Luria-Bertani media containing 100 µg/ml ampicillin at 37 $^{\circ}$C, and protein expression was induced at OD_{595} 0.6 by addition of 0.5 mM IPTG, then the culture was grown for 16 hr at 15 $^{\circ}$C. Cell pellets were harvested

by centrifugation at 4000 x *g* for 15 min. Cells were resuspended in 20 ml lysis buffer (50 mM sodium phosphate pH 8.0 containing 300 mM NaCl, 10 mM imidazole, 1 mM PMSF), cells lysed using a Constant system cell disruptor, then cell debris pelleted by centrifugation at 10,000 x *g* for 30 min. The supernatant was loaded onto a Ni-NTA resin FPLC column (HisTrap, 1 ml volume) pre-equilibrated with lysis buffer, then washed with 100 ml wash buffer (50 mM sodium phosphate pH 8.0 containing 300 mM NaCl, 20 mM imidazole). Protein was eluted by 7 ml elution buffer (50 mM sodium phosphate pH 8.0 containing 300 mM NaCl, 250 mM imidazole) at a flow rate of 0.5 ml/min. The eluted protein was subjected to buffer exchange using a PD-10 gel filtration column into 10 ml wash buffer (50 mM sodium phosphate pH 8.0 containing 300 mM NaCl, 20 mM imidazole). In order to remove the His_6 tag, the purified protein was incubated with recombinant TEV protease (1:1 molar ratio) for 16 hr at room temperature, then applied again to a Ni-NTA FPLC column, and eluted with wash buffer and elution buffer as described above. The untagged recombinant TfuDyP protein was eluted in the flow-through fraction (25 ml). The presence of recombinant TfuDyP was analysed by SDS polyacrylamide gel electrophoresis. The purified enzyme was subjected to buffer exchange using a PD-10 gel filtration column into 20 mM MOPS buffer pH 7.0 containing 80 mM NaCl.

Heme reconstitution was carried out by addition of hemin (25 mg/ml in DMSO) in a 2:1 molar ratio, incubation for 2 hr at room temperature, then centrifugation (10,000 x *g*, 10 min) to remove excess hemin. The sample was then subjected to buffer exchange using a PD-10 gel filtration column into 20 mM MOPS buffer pH 7.0 containing 80 mM NaCl, dialysed against the same buffer, then concentrated using a 10 kDa Amicon centricon device.

Steady state kinetic assays

Steady-state kinetic assays were carried out in 100 mM sodium acetate buffer pH 5.5 at 25 °C in triplicate using a Cary 1 spectrophotometer. Kinetic parameters were determined by non-linear curve fitting using Graphpad Prism 5 software. Oxidation of 2,4-dichlorophenol (DCP) was

carried out in the presence of 1 mM hydrogen peroxide, monitoring at 510 nm (ε 18,000 $M^{-1}cm^{-1}$) [10]. Oxidation of ABTS (2,2'-azino-bis(3-ethylbenzothiazoline-6-sulphonic acid) was carried out in the presence of 1 mM hydrogen peroxide, monitoring at 420 nm (ε 36,000 $M^{-1}cm^{-1}$) [7]. Oxidation of pyrogallol was carried out in the presence of 1 mM hydrogen peroxide, monitoring at 430 nm (ε 2,470 $M^{-1}cm^{-1}$) [7]. Oxidation of phenol was carried out in the presence of 1 mM hydrogen peroxide, monitoring at 505 nm (ε 7,100 $M^{-1}cm^{-1}$) [15]. Oxidation of guaiacol was carried out in the presence of 1 mM hydrogen peroxide, monitoring at 465 nm (ε 26,600 $M^{-1}cm^{-1}$) [16]. Oxidation of Reactive Blue 4 was carried out in the presence of 1 mM hydrogen peroxide, monitoring at 610 nm (ε 4,200 $M^{-1}cm^{-1}$) [7]. Oxidation of alkali Kraft lignin (Sigma Aldrich, catalogue number 471003) was carried out in the presence of 1 mM hydrogen peroxide, monitoring at 465 nm [9]. For all of the substrates, background oxidation in the presence of hydrogen peroxide was found to be very low, <0.5% of the enzyme-catalysed rates.

Pre-steady state kinetic assay

Stopped flow experiments were carried out on an Applied Photophysics SX18MV apparatus at 25 °C, mixing 5 µM recombinant TfuDyP with 5 µM hydrogen peroxide in 100 mM sodium acetate buffer pH 5.5. Apparent first order k_{obs} rate constants were determined by curve fitting using the machine software.

Assay of β-aryl ether lignin model compound

Guaiacylglycerol-β-guaiacyl ether (Tokyo chemical industry, 5 mg) was dissolved in acetone (0.2 ml), to which was added 2.8 ml 100 mM sodium acetate buffer pH 6.0. Recombinant TfuDyP (100 µl, 1 mg/ml) was added, followed by hydrogen peroxide (1 mM final concentration), and the solution was incubated for 1 hr at 30 °C. A 0.5 ml aliquot was removed, and protein precipitated by addition of trichloroacetic acid (100 % w/v, 50 µl), followed by centrifugation (microcentrifuge, 5 min). HPLC analysis was carried out using a Phenomenex Luna 5 µm C_{18}

reverse phase column on a Hewlett-Packard Series 1100 analyzer, at a flow rate of 0.5 ml/min, monitoring at 310 nm. The gradient was as follows: 20-30% methanol/water over 5 min; 30-50% methanol/water over 7 min; 50-80% methanol/water over 14 min.

Crystallisation and structure determination

Purified recombinant TfuDyP (15 mg/ml) in 20 mM MOPS buffer pH 7.5 was crystallised using conditions H2-H5 of the PACT Premier HT-96 crystallization screen (Molecular Dimensions) containing 20% w/v PEG 3350, 100 mM bis tris propane pH 8.5 and either 0.2 M sodium bromide or 0.2 M sodium iodide or 0.2 M potassium thiocyanate or 0.2 M sodium nitrate. Protein crystals (250 x 250 μm) were then grown using the hanging drop method in 20-22.5% PEG 3350, 100 mM bis tris propane pH 8.5 containing either 0.2 M sodium bromide or 0.2 M potassium thiocyanate. Crystals were cryo-protected using LV cryo oil (MiTeGen) and flash-frozen in liquid nitrogen.

X-ray diffraction data were collected to 1.7 Å at beam line I24 at Diamond Light Source using a Pilatus 6M-F detector and an X-ray wavelength of 0.97903 Å. Data were indexed and scaled using XDS [17]. Further data handling was carried out using the CCP4 software package [18]. Molecular replacement was carried out using the *Thermobifida cellulosilytica* DyP-type peroxidase (PDB code 4GS1) as a search model using PHASER [19]. Refinement of the structure was carried out by alternate cycles of REFMAC5 [20] and manual refitting using O [21]. Water molecules were added to the atomic model automatically using ARP [22] at positions of large positive peaks in the difference electron density, only at places where the resulting water molecule fell into an appropriate hydrogen-bonding environment. Refinement of the structure was carried out using non-crystallographic symmetry restraints and in the last steps of refinement all of the non-crystallographic symmetry restraints were released. The crystallographic asymmetric unit contains a homodimer and the polypeptide chain could be unambiguously traced in between residues 10-278 and 293-391 for each chain. Data collection and refinement statistics are given in Table 3.

Site-directed mutagenesis

Site-directed mutagenesis was performed for selected amino acids using the QuikChange II XL Site-Directed Mutagenesis Kit (Agilent), using the manufacturer's instructions. The mutagenesis primers were as follows: D203A forward 5'-TGGCGGTGCCGGCGATCTGCCCC-3', reverse 5'-GGGGCAGATCGCCGGCACCGCCA-3'; R315Q forward 5-AGCTGTAGCCGCGCTGGAACATGCGGGC-3', reverse 5'-GCCCGCATGTTCCAGCGCGGCTACAGCT-3'; F336A forward 5'-CTTGCCAGGCCATGGCGAGCAGTCCGGCGT-3', reverse 5'-ACGCCGGACTGCTCGCCATGGCCTGGCAAG-3'. The sequence of each mutated gene was checked by DNA sequencing, and the mutant gene expressed as described above for the wild type TfuDyP.

Results

Expression, purification and steady-state kinetic characterisation of TfuDyP

Recombinant TfuDyP was overproduced in *E. coli* BL21 as a His$_6$ fusion protein with an N-terminal 40-amino acid putative Tat signal sequence [16] removed. The enzyme was purified by nickel affinity chromatography, and the fusion tag removed using TEV protease, yielding purified protein largely free of contaminants (see Supporting Information Figure S1). The heme cofactor was reconstituted by addition of hemin in DMSO solution, followed by gel filtration chromatography, giving holoenzyme with a Soret band at 404 nm (see Supporting Information Figure S2), with an observed R$_z$ ratio of 1.12. The yield of purified enzyme was 9 mg/litre cell culture.

The pH/rate profile of the recombinant enzyme was determined using 2,4-dichlorophenol (DCP) as substrate, as shown in Figure 1A. Van Bloois *et al* previously reported that TfuDyP had activity for oxidation of Reactive Blue 19 only at pH 3.0-4.5 [16], but using 2,4-dichlorophenol we observed activity at pH 4-8. Optimum activity was observed at pH 5.0-5.5, with inflexions at pH 4.0

and 7.2. The temperature-rate profile was also determined using DCP as substrate, as shown in Figure 1B, showing optimum activity in the range 45-60 $^{\circ}$C.

Figure 1. pH/rate (A) and temperature/rate (B) profiles for TfuDyP

TfuDyP was assayed against a range of substrates using UV-vis assays, the steady-state kinetic parameters are shown in Table 1 (see Supporting Information Figure S3 for original data). Van Bloois *et al* previously reported a k_{cat} of 10 s^{-1} for Reactive Blue 19 at pH 3.5, and a relative activity of 29.5% for Reactive Blue 4 [16], compared with our k_{cat} value of 1.9 s^{-1} for Reactive Blue 4 at pH 5.5. The substrate with the highest k_{cat} value (28 s^{-1}) in our study was the peroxidase substrate ABTS. Activity was also observed for phenol, pyrogallol, and 2,4-dichlorophenol, in the range k_{cat}/K_m 500-1000 M^{-1}s^{-1}, but no activity was observed with guaiacol. For decolorization of Reactive Blue 4, TfuDyP showed higher k_{cat} than *R. jostii* DypA or DyPB [7].

Using alkali Kraft lignin as substrate, we observed a change in absorbance at 465 nm, as previously observed for *R. jostii* DypB [9] and *P. fluorescens* Dyp1B [15], which showed saturation kinetic behaviour versus substrate concentration (see Supporting Information Figure S3), indicating that some part of the Kraft lignin is binding to the enzyme and undergoing oxidation. Using an average molecular weight of 10,000 Da, an apparent K_M value of 10 µM can be deduced, compared with 20 µM for *R. jostii* DypB [9] and 6 µM for *P. fluorescens* DyP1B [15]. The magnitude of this apparent K_M should be interpreted with caution, because the substrate is heterogeneous, and the enzyme probably interacts only with a part of the substrate. TfuDyP showed no activity for Mn^{2+} oxidation, and showed no reactivity towards wheat straw lignocellulose, via HPLC analysis.

The reaction of TfuDyP with hydrogen peroxide was analysed using stopped flow kinetic analysis. At pH 5.5, equimolar mixing of 5 µM TfuDyP with 5 µM H$_2$O$_2$ resulted in the decay of the Soret band at 404 nm within 400 ms, giving a compound I intermediate with λ_{max} 404 nm, and changes in absorbance of a weak absorption at 500-550 nm, as shown in Figure 2A. By monitoring

8

transient kinetics at 404 nm at a range of hydrogen peroxide concentrations, a second order rate constant of 5.5×10^4 $M^{-1}s^{-1}$ was measured for compound I formation.

Figure 2. Pre-steady state kinetic behaviour of TfuDyP.

Oxidation of β-aryl ether lignin model compound

Dimeric β-aryl ether lignin model compounds have been frequently used to study the action of fungal lignin-oxidising enzymes [23], and bacterial DyPs [9,10] and laccases [24]. TfuDyP was incubated with guaiacylglycerol-β-guaiacyl ether (**1**) at 1.6 mg/ml concentration in 100 mM sodium acetate buffer pH 6.0 in the presence of 1 mM hydrogen peroxide. Monitoring by reverse phase HPLC revealed the formation of a new product at retention time 16 min, as shown in Figure 3B. The peak was not formed in the absence of enzyme or hydrogen peroxide. Analysis of this peak by electrospray mass spectrometry gave a sodiated ion at *m/z* 661.2255, consistent with molecular formula $C_{34}H_{38}O_{12}Na$ (calculated 661.2255). MS-MS fragmentation of this species gave a major fragment at *m/z* 343.2, consistent with the structure of the β-aryl ether monomer (MNa 343.2), implying that oxidative dimerization of the model compound had taken place. The most likely structure, formed by C-C coupling of the free phenolic coupling unit in (**1**) would be the biphenyl structure shown in Figure 3A, though other isomeric structures are also possible. As shown in Table 1, TfuDyP also showed oxidation activity towards Kraft lignin.

Figure 3. Oxidation of β-aryl ether lignin model compound oxidation by TfuDyP.

Crystal structure determination

We noticed that an independently determined structure of a similar enzyme from *Thermobifida cellulosilytica* (PDB code 4GS1, released in September 2013) has been deposited, but no further analysis and publication have followed this structure. Crystallisation of purified TfuDyP

9

was achieved in 100 mM Bis Tris propane buffer pH 8.5 containing 20% (w/v) PEG 3350 and 0.2 M sodium bromide or potassium thiocyanate. X-ray diffraction data were collected to 1.8 Å, and the structure was solved by molecular replacement using the deposited co-ordinates for *Thermobifida cellulosilytica* DyP-type peroxidase (PDB code 4GS1). The tertiary structure shown in Figure 4A consists of a homodimer of subunits containing a four-stranded antiparallel β-sheet βαββαβ motif within a ferredoxin-like fold, similar to the structures of DyPs from *B. adusta* [3] and *R. jostii* RHA1 [7]. The heme cofactor shown in Figure 4B was ligated by proximal His-299, and on the distal face were located Asp-203 and Arg-315, as found in other DyP peroxidase active sites [3,7]. Phe-336 was also located on the distal face of the heme cofactor, 3.6 Å above the distal face of the porphyrin ring.

A diatomic ligand was identified at 1.8 Å resolution on the distal face of the heme cofactor, 3.5 Å from the carboxylate group of Asp-203, and 5.8 Å from the ε-nitrogen atom of Arg-315. Although the resting state of the enzyme contains iron (III), it is known that prolonged X-ray exposure can cause photoreduction to iron (II) [25-27], which could bind dioxygen as a ligand, hence we interpret the diatomic ligand as an iron (II)-dioxygen or iron (III)-superoxide species.

Figure 4. Crystal structure of *T. fusca* DyP.

Analysis of the structure using MOLE 2.0 software revealed the presence of two tunnels in the structure providing access to the heme cofactor. The larger tunnel (see Figure 4C) provides access to the distal face of the heme cofactor, lined by Asp-203, Gly-317, Ser-319, Leu-334, Phe-336, Arg-196, Tyr-318, Phe-181, Arg-183, Pro-195, Arg-315, Arg-316 and Ala-39. The smaller tunnel (see Supporting Information Figure S4) provides access to the proximal face of heme, lined by Ile-243, His-367, Ile-365, Gln-351, Leu-354, Asn-362, Thr-133, Ile-362, and Arg-366. The function of the smaller channel is uncertain, but it might provide access for hydrogen peroxide or

act as a proton channel. Attempts to co-crystallise TfuDyP with phenolic substrates, lignin model compounds and polymeric lignin were unsuccessful (data not shown).

Investigation of active site residues by site-directed mutagenesis

In order to investigate the function of the amino acid residues on the distal face of the heme cofactor, site-directed mutant enzymes D203A, R315Q and F336A were generated by Quikchange PCR mutagenesis, as described in the Materials and Methods. Van Bloois have previously mutated Asp-203 and the proximal heme ligand His-299, and reported 0.7% and 3% activity respectively for Reactive Blue 19 with these mutant enzymes [16]. Each mutant enzyme was expressed, purified and reconstituted in a similar way to the wild-type enzyme (see Supporting Information Figure S6), in similar overall yield. Each mutant enzyme was kinetically characterised using ABTS and phenol as substrates, and steady state kinetic parameters measured, as shown in Table 2.

Mutant D203A showed no activity towards phenol as substrate, but showed low activity towards ABTS, reduced 28-fold in k_{cat} compared with wild-type TfuDyP, and 36-fold reduced k_{cat} for hydrogen peroxide. Mutant R315Q showed no activity towards phenol, and no measurable activity towards ABTS at 1 mM hydrogen peroxide, but low levels of activity were measurable at high concentrations of hydrogen peroxide (K_M 8.6 mM). Mutant F336A showed essentially identical activity towards phenol as the wild-type enzyme, and 2-fold higher k_{cat} for ABTS oxidation.

Conclusions

Thermobifida fusca, an active cellulose degrader, has been previously shown to contain a DyP-ype peroxidase, which shows thermostable activity towards anthraquinone dyes such as Reactive Blue 19 and Reactive Blue 4, and modest activity towards phenols such as guaiacol and 2,6-dimethoxyphenol [16]. We have shown that recombinant TfuDyP has oxidation activity towards Kraft lignin and a β-aryl ether lignin model compound, hence identifying a further bacterial DyP

with activity towards lignin substrates, as previously observed for *R. jostii* RHA1 DypB [9] and *P. fluorescens* Pf-5 DyP1B [15]. However, unlike *R. jostii* DyPB and *P. fluorescens* DyP1B, TfuDyP shows no activity for Mn^{2+} oxidation, hence the lignin oxidation activity of TfuDyP must be due either to direct oxidation by the heme cofactor, or electron transfer via a surface redox-active residue, as is known for fungal lignin peroxidase [28]. The lack of Mn^{2+} oxidation activity has also been observed in other A-type DyP enzymes [7,15].

The observed dimerization of β-aryl ether lignin model compound is an example of "lignin repolymerisation" behaviour, whereby the same enzymes that can depolymerise lignin via phenoxy radical formation also cause polymerisation via phenoxy radical coupling. This phenomenon has been observed for *R. jostii* RHA1 DyPB [9], and also for bacterial laccases from *Streptomyces coelicolor* and *S. viridosporus* T7A [24], and represents a significant challenge for the use of these enzymes *in vitro* for lignin depolymerisation, though this phenomenon is generally not observed in living systems, so there may be mechanisms to combat this phenomenon *in vivo*.

The structure of TfuDyP was solved at 1.8 Å, and shows a ferredoxin-type fold that is similar to structures of other DyPs from bacteria [7, 10] and fungi [3, 29]. Similar to other DyPs [3], TfuDyP contains Asp-203 and Arg-315 on the distal face of the heme cofactor, which are both important for catalytic activity, and the catalytic Asp residue is found in a GxxDG sequence motif, as noted in other DyPs [3]. The TfuDyP structure contains a diatomic ligand bound to the distal face of the heme cofactor, which we presume arises from photoreduction of the iron centre during X-ray data collection, and capturing of dioxygen [25-27]. The position of the diatomic ligand therefore provides some indication of the positioning of the hydrogen peroxide substrate during catalysis. Since the distal oxygen of the diatomic ligand is hydrogen-bonded to Asp-203 at a distance of 3.5 Å, we propose that Asp-203 acts as a proton donor to protonate hydrogen peroxide in the generation of the compound I reaction intermediate, as originally proposed for *B. adusta* DyP [3].

The lack of activity of the R315Q mutant enzyme demonstrates that Arg-315 is also important for catalytic function: it is positioned close to the diatomic ligand, therefore we suggest

that Arg-315 may stabilise the compound I intermediate via hydrogen bonding [30]. In *B. adusta* DyP, replacement of Asp-171 led to 3,000-fold loss of activity [3], whereas in *R. jostii* DyPB, replacement of Asp-153 by Ala gave a more active mutant enzyme [31], hence the observed effects of active site replacements vary considerably between enzymes, but our data is more consistent with the observations made for *B. adusta* DyP [3]. The third distal residue Phe-336 is not essential for catalysis, in fact the F336A mutant has higher activity towards ABTS, perhaps due to a larger substrate cavity in this mutant enzyme.

The conformation of substrates bound to the TfuDyP active site is uncertain, and attempts to co-crystallise phenolic substrates and lignin model compounds with TfuDyP were unsuccessful. We have carried out molecular docking of several substrates to the TfuDyP structure using AutoDock-vina and GOLD docking software, which has suggested a possible bound conformation involving a hydrogen bond between the hydroxyl group of the ligand and a heme propionate sidechain (see Supporting Information Figure S5) that might direct the site of oxidation by the enzyme. Ogola *et al* have reported docking of guaiacol and Reactive Blue 5 to the active site of *Anabaena* DyP, where they observed a bound conformation on the distal face of the heme cofactor [32]. The thermal stability of this enzyme [16] makes it potentially attractive for future biotechnological applications.

References

1. Y. Sugano, Cell. Mol. Life Sci. 66 (2009) 1387-1403.

2. T. Yoshida and Y. Sugano, Arch. Biochem. Biophys. 574 (2015) 49-55.

3. Y. Sugano, R. Muramatsu, A. Ichiyanagi, T. Sato, and M. Shoda, J. Biol. Chem. 282 (2007) 36652-36658.

4. S.J. Kim and M. Shoda, Appl. Environ. Microbiol. 65 (1999) 1029-1035.

5. H.J.O. Ogola, T. Kamiike, N. Hashimoto, H. Ashida, T. Ishikawa, H. Shibata, and Y. Sawa, Appl. Environ. Microbiol. 75 (2009) 7509-7518.

6. A. Santos, S. Mendes, V. Brissos, and L.O. Martins, Appl. Microbiol. Biotechnol. 98 (2014) 2053-2065.

7. J.N. Roberts, R. Singh, J.C. Grigg, M.E.P. Murphy, T.D.H. Bugg, and L.D. Eltis, Biochemistry, 50 (2011) 5108-5119.

8. S. Letoffé, G. Heuck, P. Delepelaire, N. Lange, and C. Wandersman, Proc. Natl. Acad. Sci. USA 106 (2009) 11719-11724.

9. M. Ahmad, J.N. Roberts, E.M. Hardiman, R. Singh, L.D. Eltis, and T.D.H. Bugg, Biochemistry 50 (2011) 5096-5107.

10. M.E. Brown, T. Barros, and M.C.Y. Chang, ACS Chem. Biol. 7 (2012) 2074-2081.

11. Y. Sugano, R. Nakano, K. Sasaki, and M. Shoda, Appl. Environ. Microbiol. 66 (2000) 1754-1758.

12. C. Liers, C. Bobeth, M. Pecyna, R. Ullrich, and M. Hofrichter, Appl. Microbiol. Biotechnol. 85 (2010) 1869-1879.

13. T.D.H. Bugg, M. Ahmad, E.M. Hardiman, and R. Singh, Curr. Opin. Biotech. 22 (2011) 394-400.

14. P.D. Sainsbury, E.M. Hardiman, M. Ahmad, H. Otani, N. Seghezzi, L.D. Eltis, and T.D.H. Bugg, ACS Chem. Biol. 8 (2013) 2151-2156.

15. R. Rahmanpour and T.D.H. Bugg, Arch. Biochem. Biophys. 574 (2015) 93-98.

16. E. Van Bloois, D.E. Torres Pazmino, R.T. Winter, and M.W. Fraaije, Appl. Microbiol. Biotechnol. 86 (2010) 1419-1430.

17. W. Kabsch, Acta Cryst. D66 (2010) 125-132.

18. Collaborative Computational Project Number 4, Acta Cryst. D50 (1994) 760-763.

19. A.J. McCoy, R.W. Grosse-Kunstleve, P.D. Adams, M.D. Winn, L.C. Storoni, and R.J. Read, J. Appl. Cryst. 40 (2007) 658-674.

20. G.N. Murshudov, P. Skubak, A.A. Lebedev, N.S. Pannu, R.A. Steiner, R.A. Nicholls, M.D. Winn, F. Long, and A.A. Vagin, Acta Cryst. D67 (2011) 355-367.

21. T.A. Jones, J.Y. Zou, S.W. Cowan, and M. Kjeldgaard, Acta Cryst. A47 (1991) 110-119.

22. A. Perrakis, R. Morris, and V.S. Lamzin, Nat. Struct. Biol. 6 (1999) 458-463.

23. T.K. Kirk and R.L. Farrell Annu. Rev. Microbiol. 41 (1987) 465-505.

24. S. Majumdar, T. Lukk, J.O. Solbiati, S. Bauer, S.K. Nair, J.E. Cronan, and J.A. Gerlt, Biochemistry 53 (2014) 4047-4058.

25. L.M. Podust, A. Ioanoviciu, and P.R. Ortiz de Montellano, Biochemistry 47 (2008) 12523-12531.

26. A. Arcovito, T. Moschetti, P. D'Angelo, G. Mancini, B. Vallone, M. Brunori, and S. Della Longa, Arch. Biochem. Biophys. 475 (2008) 7-13.

27. T. Beitlich, K. Kühnel, C. Schulz-Briese, R.L. Shoeman, and I. Schlichting, J. Synchrotron Radiation 14 (2007) 11-23.

28. A.T. Smith, W.A. Doyle, P. Dorlet, and A. Ivancich, Proc. Natl. Acad. Sci. USA 106 (2009) 16084-16089.

29. E. Strittmatter, C. Liers, R. Ullrich, S. Wachter, M. Hofrichter, D.A. Plattner, and K.J. Piontek, Biol. Chem. 288 (2013) 4095-4102.

30. A. N. P. Hiner, E. L. Raven, R. N. F. Thorneley, F. Garcia-Canovas, and J. N. Rodriguez-Lopez, J. Inorg. Biochem. 91 (2002) 27-34.

31. R. Singh, J.C. Grigg, Z. Armstrong, M.E.P. Murphy, and L.D. Eltis, J. Biol. Chem. 287 (2012) 10623-10630.

32. H.J.O. Ogola, T. Kamiike, N. Hashimoto, H. Ashida, T. Ishikawa, H. Shibata, and Y. Sawa, Appl. Environ. Microbiol. 75 (2009) 7509-7518.

33. W.L. DeLano (2002). The PyMOL User's Manual, DeLano Scientific, Palo Alto, CA.

Table 1. Steady-state kinetic data for TfuDyP. Assay conditions are described in Materials and Methods. NA, no activity. [a] Using ABTS as substrate.

	TfuDyP		
Substrate	**K_M (mM)**	**k_{cat} (s^{-1})**	**k_{cat}/K_M ($M^{-1}s^{-1}$)**
ABTS	0.86±0.07	28.1±1	3.26 x 10^4
H_2O_2[a]	0.082±0.003	36.3±0.3	4.39 x 10^5
Mn^{2+}	NA	NA	NA
2,4-dichlorophenol	5.51±0.5	2.86±0.1	0.518 x 10^3
Phenol	0.126±0.01	0.136±0.03	1.077 x 10^3
Guaiacol	NA	NA	NA
Pyrogallol	11.29±1	6.63±0.25	0.587 x 10^3
Reactive Blue 4	0.179±0.01	1.88 ±0.07	10.46 x 10^3

Table 2. Steady state kinetic parameters measured for wild-type, D203A, R315Q and F336A mutant TfuDyP enzymes. Assay conditions described in Materials and Methods. [a] No activity at 1mM hydrogen peroxide, [b] Activity measured at above 1mM hydrogen peroxide.

	ABTS			**H_2O_2**			**Phenol**		
	K_M (mM)	k_{cat} (s^{-1})	k_{cat}/K_M ($M^{-1}s^{-1}$)	K_M (mM)	k_{cat} (s^{-1})	k_{cat}/K_M ($M^{-1}s^{-1}$)	K_M (mM)	k_{cat} (s^{-1})	k_{cat}/K_M ($M^{-1}s^{-1}$)
TfuDyP WT	0.86±0.07	28.1±1	3.26×10^4	0.082±0.01	36.3±0.39	4.40×10^5	0.126±0.01	0.136±0.0	1080
D203A mutant	0.122±0.01	1.01±0.01	8.27×10^3	0.066±0.00	1.3±0.02	1.9×10^4	No activity	No activity	No activity
R315Q mutant	No Activity [a]	No activity	No activity	8.6±0.82 [b]	8.26±0.39	960	No activity	No activity	No activity
F336A mutant	1.13±0.12	66.5±3.5	5.88×10^4	0.053±0.00	30.51±0.48	5.72×10^5	0.118±0.01	0.137±0.0	1160

Table 3. Crystallographic data collection and refinement statistics

Data collection	
Unit cell a,b,c (Å),	a= 143.36, b= 110.21, c=46.73
Space group	$P2_12_12$
Resolution (Å)	42-1.8 (1.9-1.8)
Observations	356,664
Unique reflections	69,391
$I/\sigma(I)$	14.7 (3.2)
R_{sym}[a]	0.074 (0.443)
Completeness (%)	99.8 (99.8)
CC(1/2)[1]	99.8 (91.8)
Refinement	
Non-hydrogen atoms	6,088 (including 2 haems with the bound oxygens & 412 waters)
R_{cryst}	0.204 (0.345)
Reflections used	66,586 (4,815)
R_{free}	0.249 (0.352)
Reflections used	2,805 (212)
R_{cryst} (all data)	0.206
Average temperature factor (Å^2)	31.4
Rmsds from ideal values	
Bonds (Å)	0.013
Angles (º)	1.6
DPI coordinate error (Å)	0.142
wwPDB ID code	5FW4

[1]Percentage of correlation between intensities from random half-datasets.

Figure Legends

Figure 1. pH/rate (A) and temperature/rate (B) profiles for *T. fusca* DyP, using DCP as substrate. Temperature-rate profile was carried out in 100 mM sodium acetate buffer pH 5.5.

Figure 2. Pre-steady state kinetic behaviour of *T. fusca* DyP. A. UV-visible scans obtained upon mixing 5 μM TfuDyP with 5 μM hydrogen peroxide in 100 mM sodium acetate buffer pH 5.5 at 4, 40, and 400 ms (inset shows expansion at 450-650 nm). B. Transient absorbance of Soret band at 404 nm, from which first-order k_{obs} was obtained from data fitting (inset plot of k_{obs} vs [H_2O_2])

Figure 3. Oxidation of β-aryl ether lignin model compound by TfuDyP. A. Proposed structure for dimerization product. B. Reverse phase HPLC analysis showing formation of oxidised product.

Figure 4. Crystal structure of *T. fusca* DyP. A. Tertiary structure of protein. B. Environment of heme cofactor, showing amino acids close to proximal and distal faces. The SIGMAA weighted 2mFo-ΔFc electron density using phases from the final model is contoured at 1.0 Å level, where s represents the RMS electron density for the unit cell. Contours more than 1.4 Å from any of the displayed atoms have been removed for clarity. Thin lines indicate hydrogen bonds. Drawn with PyMOL [33]. C. Entrance to active site cavity via larger tunnel.
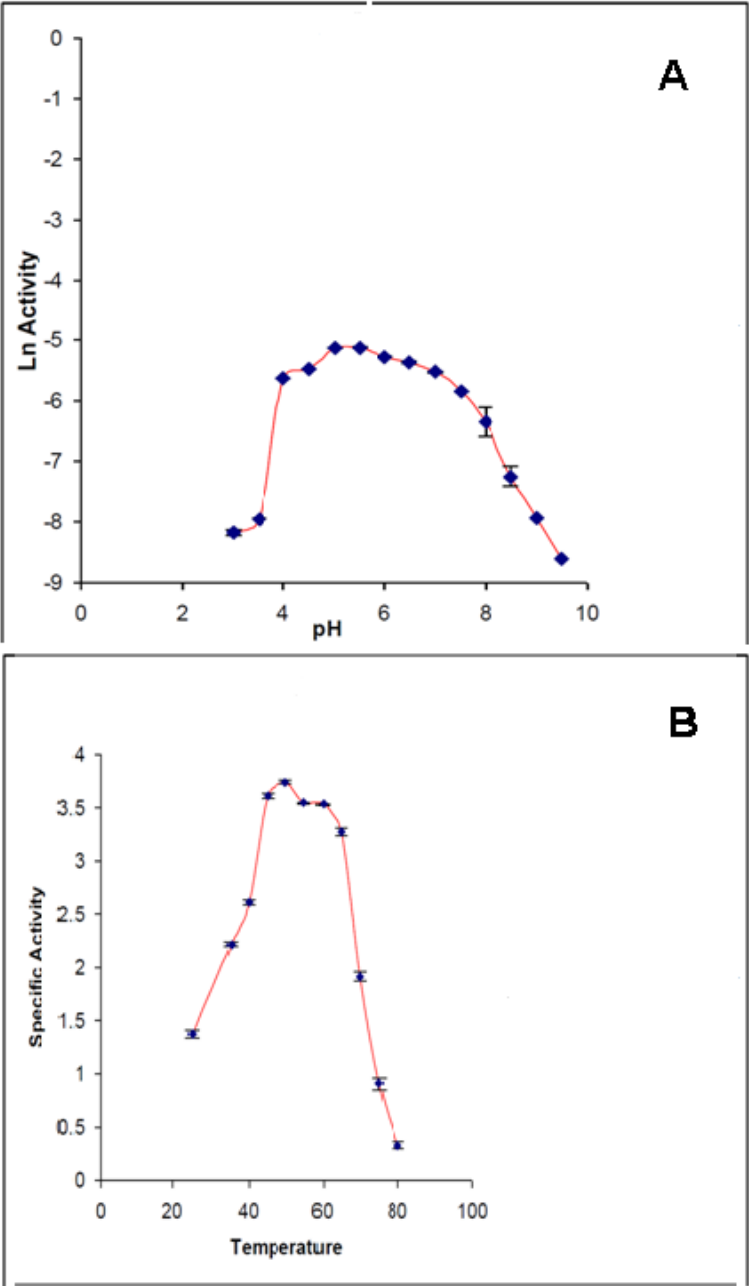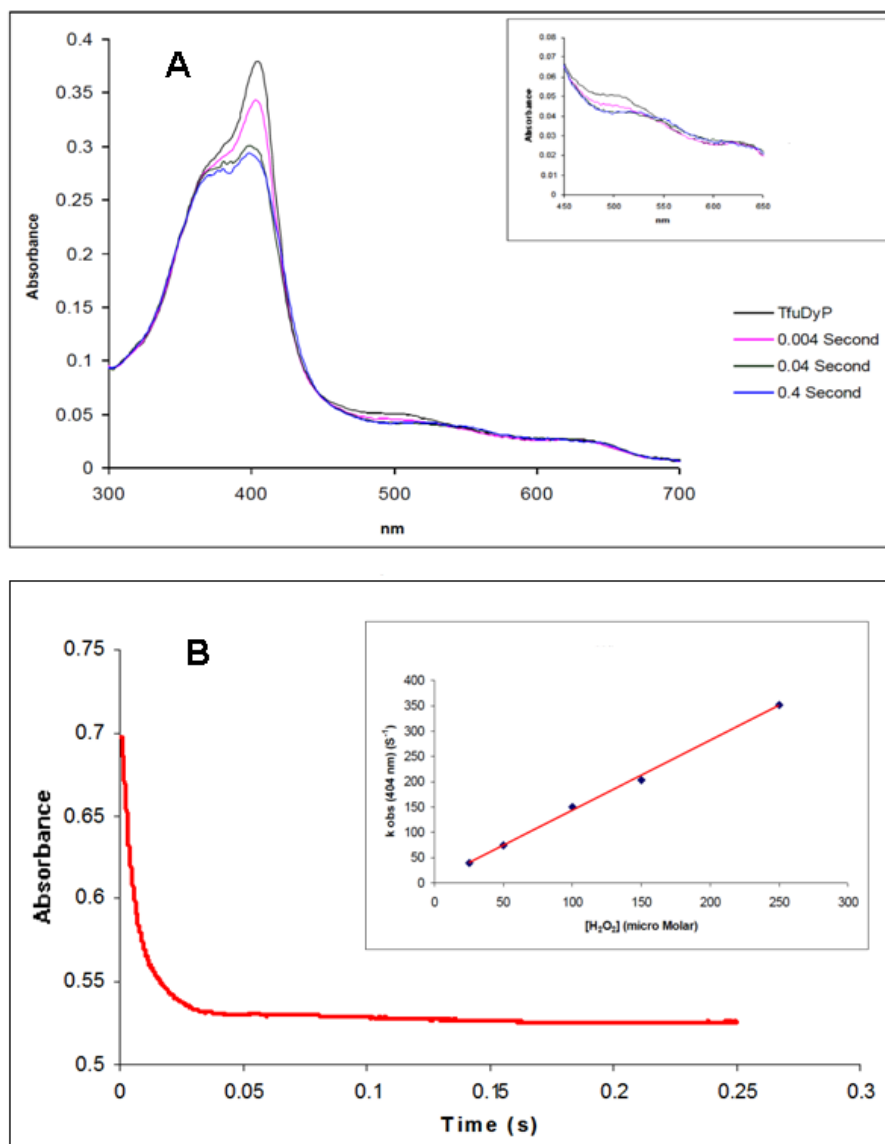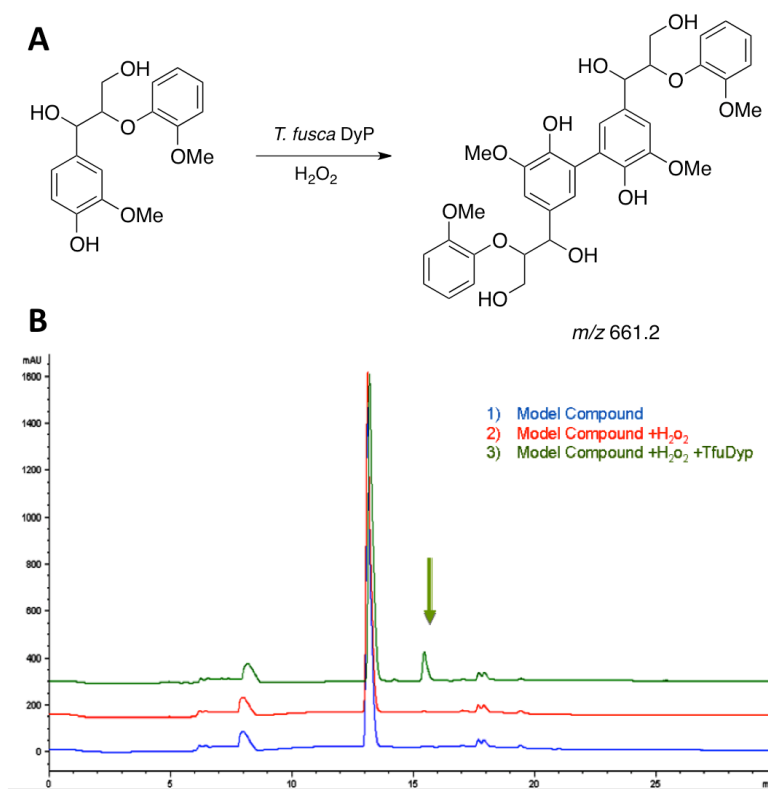
Figure 1

Figure 2

Figure 3

Figure 4